Aggregation of V2H Systems to Participate in Regulation Market

Hikari Nakano, Ikumi Nawata, Shinkichi Inagaki, *Member, IEEE*, Akihiko Kawashima, *Member, IEEE*, Tatsuya Suzuki, *Member, IEEE*, Akira Ito, *Member, IEEE*, and Willett Kempton, *Member, IEEE*

***Abstract*— Ancillary services are becoming an indispensable tool for maintaining power grid stability due to the increasing adoption of renewable energy resources, many of which (e.g., wind and solar power) are inherently variable. Some energy resources, such as electric vehicles (EVs), have a significant potential for providing their own ancillary services and creating ancillary service markets in smart electric grids. The installation convenience of EVs and plug-in hybrid vehicles (PHVs) has made them the target of many studies. In previous works, the grid-integrated-vehicle (GIV) mechanisms are recognized as a suitable approach to exploit EVs and PHVs for ancillary service markets, particularly regulation markets, which require fast responses. It is important to consider individual consumption behavior (e.g., vehicle usage and energy consumption) in selecting optimal operational points of EV and PHV for maximizing resource effectiveness and user profit. There is, however, currently no mechanism that takes the individual consumption behavior of market participants into account. In this article, a new vehicle-to-home (V2H) aggregator is proposed, which allows individuals to participate in a regulation market using the in-vehicle batteries of their EVs or PHVs. The results show that the proposed V2H aggregator can successfully supply predictable power to the power grid and maximize the profits of individual market participants.**

***Note to Practitioners*—This article proposes an architecture of home energy management systems (HEMSs) with electric vehicles (EVs) and plug-in hybrid vehicles (PHVs) to participate in a regulation market using the in-vehicle batteries. Ancillary services are the mechanism for the power grid to ensure the quality of electricity. The proposed architecture is composed of two stages: 1) calculation of the charge and discharge profiles considering minimizing the electricity charge at home and maximizing the capacity to provide for ancillary services and 2) real-time control of charging and discharging the in-vehicle batteries to follow the regulation signal provided from the manager of ancillary services. The simulation result shows the estimated benefit of the aggregator obtained by the trade in the market and the precision of HEMSs' charging and discharging to follow the request signal.**

***Index Terms*— Ancillary service, distributed decision making, energy management system (EMS), model predictive control (MPC).**

NOMENCLATURE

$T = 48$	Time period to be considered in model predictive scheduling of charge/discharge.
$t \in [0, T-1]$	Discretized time step used in model predictive scheduling ($\Delta t = 30$ min).
$L = 900$	Total number of regulation signals received by the aggregator in Δt.
$\ell \in [0, L-1]$	Time step of receiving the regulation signals ($\Delta \ell = 2$ s).
$m \in \{0, 1, 2, \ldots\}$	Repeat count of recursive procedure in the balancing control.
H	Set of homes equipping an HEMS.
$H'(t) \in H$	Set of homes with vehicle parked at home at t.
$\tilde{W}_h^+(k\|t) \geq 0$	Predicted electric power consumed in home h at time step k predicted at t (kW).
$\tilde{W}_h^-(k\|t) \leq 0$	Predicted electric power generated in home h at time step k predicted at t (kW).
$\tilde{P}_h^{\text{cons}}(k\|t) \geq 0$	Consumed electric power of vehicle by driving at time step k predicted at t (kW).
$F^+(t) > 0$	Purchase price of electric energy at t (JPY/kWh).
$F^-(t) > 0$	Sale price of electric energy at t (JPY/kWh).
$\tilde{\Gamma}_h(k\|t) \in \{0,1\}$	Binary variable indicating whether the vehicle owned by home h is available in the HEMS at time step k predicted at t, where $\tilde{\Gamma}_h(k\|t) = 0$ indicates that the vehicle is connected to the home and 1 indicates that the vehicle is used for transportation.

Manuscript received December 3, 2019; revised March 17, 2020; accepted May 12, 2020. This article was recommended for publication by Associate Editor J. R. Morrison and Lead Guest Editor I. Si upon evaluation of the reviewers' comments. This work was supported by Japan Science and Technology Agency (JST), Core Research for Evolutional Science and Technology (CREST) (Creation of Fundamental Theory and Technology to Establish a Cooperative Distributed Energy Management System and Integration of Technologies Across Broad Disciplines Toward Social Application). *(Corresponding author: Shinkichi Inagaki.)*

Hikari Nakano is with Nuvve Corporation, San Diego, CA 92106 USA (e-mail: hikari@nuvve.com).

Ikumi Nawata is with the Graduate School of Engineering, Nagoya University, Nagoya 464-8603, Japan (e-mail: i_nawata@nuem.nagoya-u.ac.jp).

Shinkichi Inagaki is with the Department of Mechatronics, Faculty of Science and Engineering, Nanzan University, Nagoya 466-8673, Japan (e-mail: inag@nanzan-u.ac.jp).

Akihiko Kawashima is with Yamato Holdings Company Ltd., Tokyo 104-0031, Japan (e-mail: a_kawashima@kuronekoyamato.co.jp).

Tatsuya Suzuki is with the Graduate School of Engineering, Nagoya University, Nagoya 464-8603, Japan, and also with JST, CREST, Tokyo 102-0076, Japan (e-mail: t_suzuki@nuem.nagoya-u.ac.jp).

Akira Ito is with Denso Corporation, Kariya 448-8661, Japan (e-mail: akira.ito.j8p@jp.denso.com).

Willett Kempton is with the ISE Lab, Center for Research in Wind, College of Earth, Ocean, and Environment, University of Delaware, Newark, DE 19716 USA (e-mail: willett@udel.edu).

Color versions of one or more of the figures in this article are available online at http://ieeexplore.ieee.org.

Digital Object Identifier 10.1109/TASE.2020.3001060

$W_h^{\max} > 0$	Upper bound of electric power in household of home h [kW].
$P_h^{\text{char}} > 0$	Upper bound of electric power for charging the in-vehicle battery from home h [kW].
$P_h^{\text{dis}} < 0$	Lower bound of electric power for discharging the in-vehicle battery to home h [kW].
$B_h(k\|t) \geq 0$	Electric energy of in-vehicle battery owned by home h at time step k planned at t [kWh].
$B_h^{\max} > 0$	Upper bound of electric energy of in-vehicle battery of home h [kWh].
$B_h^{\min} \geq 0$	Lower bound of electric energy of in-vehicle battery of home h [kWh].
$B_h^{\text{ref}} \geq 0$	Lower bound of electric energy of in-vehicle battery of home h at departure time [kWh].
$B_h^0(t)$	Electric energy of in-vehicle battery of home h observed or estimated at t [kWh].
$\eta^{\bullet} > 0$	$\bullet \in$ {char, dis}, coefficient of {charge, discharge}.
$P^{\text{st}} \geq 0$	Standby power of power conditioner system [kW].
$P_h^s(k\|t)$	$s \in$ {up, low}, charging or discharging electric power of vehicle of home h by model predictive charge/discharge scheduler at time step k planned at t [kW], where positive indicates charge of the in-vehicle battery and negative indicates discharge of the in-vehicle battery.
$P_h^{\text{POP}}(k\|t)$	Preferred operating point of charging or discharging electric power [kW].
$\alpha > 0$	Coefficient of penalty for battery degradation.
$\beta > 0$	Coefficient of incentive and penalty for increasing SoC.
$\mu(\ell; t)$	Lagrange multiplier at time step ℓ of t.
$w_h^+(\ell; t) \geq 0$	Consumed electricity power of home h at time step ℓ of t [kWh].
$w_h^-(\ell; t) \leq 0$	Generated electricity power of home h at time step ℓ of t [kWh].
$p_h(\ell; t)$	Charging or discharging electric power of vehicle of home h calculated by the balancing controller at time step ℓ of t [kW].
$P^s(t)$	$s \in$ {up, low}, sum of $P_h^s(0\|t)$ for $h \in H'(t)$ which is used by an aggregator to bid to the regulation market [kW].
$\tilde{W}^{\text{POP}}(t)$	Total net electric power for 30 min to be purchased from the grid by the houses $h \in H'(t)$.
$p^{\text{as}}(t)$	Assigned regulation signal that is sent every 30 min from the TSO to the aggregator.
$p^{\text{req}}(l; t)$	Regulation control signal that is sent every 2 s from the TSO to the aggregator.
$p^{\text{reg}}(l; t)$	Sum of the assigned regulation signal and the regulation control signal.

I. Introduction

ANCILLARY services ensure the stability and security of electric grids by minimizing the occurrences of accidents, such as blackouts or short-term frequency changes. Several types of ancillary services exist and are specialized to handle specific issues that arise during the operation of an electric grid.

There are three main types of ancillary services. The first ancillary service is the scheduling and dispatch service internal to an electric grid operator. This type of service operates in a timescale of days and is responsible for scheduling and coordinating the generation and transmission units on the electric grid. The second type of ancillary service is spinning reserve. Spinning reserve responds to sudden outages and increases in power load by starting up reserve power resources within 10 s to supply the required power to the electric grid. Third common type of ancillary service is frequency regulation. Frequency regulation balances power supply and demand instantaneously and corrects small frequency deviations within a few seconds. Because of its characteristic of faster response times, frequency regulation generally requires a highly responsive outside energy source.

Recently, ancillary services have become more indispensable for electricity grids due to the increased adoption of variable power generation from renewable energy resources, such as photovoltaics (PVs) and wind energy power plants [1], [2]. In many countries, market-based ancillary services are operated in which energy resources participate by bidding their capacity as buffers [3]–[5]. In USA, ancillary service markets are operated by independent system operators (ISOs) or regional transmission organizations (RTOs), such as the California Independent System Operator (CAISO), the Midcontinent Independent System Operator (MISO), the Southwest Power Pool (SPP), or the Pennsylvania-New Jersey-Maryland Interconnection (PJM) [6]. A survey shows that the market size of these transmission system operators (TSOs) grew up to more than 2000 MW of total capacity by 2014 [7]. Due to the rapid growth of these markets, there has been an interest in studying how energy resources can participate in ancillary markets efficiently and a number of strategies have been developed [8]–[12].

In Japan, ancillary services are provided only internally by vertically integrated electric companies. Electricity deregulation from 2016 allows the Japanese electric system to introduce open market ancillary services. In fact, the share of electricity from new power producers and suppliers (PPSs) increased by 7% of total share of electricity within two years after the electricity deregulation started [13]. For this reason, it is important to investigate new strategies for effective participation in the ancillary service markets to effectively include newer energy resources for the future electric system in Japan.

Previously, the authors have proposed a home energy management system (HEMS), which was operated by model predictive control (MPC) using in-vehicle batteries of electric vehicles (EVs) or plug-in hybrid vehicles (PHVs) [14]–[18]. In [14], a method to plan and control charging and discharging of EV and PHV batteries to minimize household electric bills over 24 h was proposed. In addition, the effectiveness of vehicle-to-home (V2H)-HEMS with a prediction of vehicle usage and energy consumption was demonstrated. In [15] and

[16], estimation methods for a profile of vehicle usage from the present time toward the future based on the Markov processes and greedy algorithm [15] or dynamic programming [16] was developed. In these articles, it has been demonstrated that the developed V2H-HEMS could automatically calculate an optimal charging and discharging profile for EV and PHV batteries and could minimize the electric bill of the household over 24 h. The system is expected to be applied for ancillary service markets by calculating the optimal bidding capacity using an MPC framework.

EV and PHV batteries have a significant potential for providing ancillary services—in particular, frequency regulation services—due to their fast response capabilities and ease of installation. According to these characteristics, several grid-integrated-vehicle (GIV) mechanisms, such as a V2G aggregator, have already been proposed [19]–[25]. In [19], a multiagent system that integrates EVs into the electricity grid was implemented and deployed. In [20], two different types of GIV mechanisms were provided and compared quantitatively in computational simulation. Al-Anbagi *et al.* [21] provided a mechanism to maximize the number of EVs that can participate in the frequency regulation market. A roadside unit (RSU) was used to increase the number of EVs to be reached out by the aggregator. Ansari *et al.* [22] demonstrated the mechanism to optimize the coordination of bidding of EV battery capacities across different ancillary service markets by a fuzzy optimization technique. They used forecast several market parameters by the ARIMA model. Gil *et al.* [23] proposed a model to maximize the profit of EVs and PHVs parking lot by participating in day-ahead energy, spinning reserve and regulation markets considering the individual contracts with PEV owners. Peng *et al.* [24] and Liu *et al.* [25] proposed V2G aggregator mechanisms that can satisfy EV driving demand.

Especially, EV and V2G aggregators based on optimization and multitime horizon controls are proposed [26]–[28] similar to the proposed architecture in this article. Vagropoulos *et al.* [26] provided a framework of EV aggregator participating in the electric energy and regulation markets based on three control levels: 1) calculation of charging power request of the vehicle fleet for 1 h; 2) dispatching the power request during 5 min to each vehicle based on priorities; and 3) real-time charging control in the period of 4 s. Wang *et al.* [27] designed and analyzed a V2G aggregator-based MPC. The aggregator derives charging and regulation control parameters that minimize the total cost of electricity fee for charging the vehicles over some time slots considering both the penalty to meet the vehicle usage and the estimated incentive from the regulation market. In [28], a regulation mechanism for matching the renewable energy supply and the power demand was proposed. It is composed of two stages: day-ahead scheduling for controllable energy plants and EV charging stations, and real-time charging control of EVs.

Although there are many literature works addressing how to design V2H-HEMS that utilizes the batteries of EVs or PHVs for HEMS, only a few works were devoted to seek the possibility of exploiting the V2H-HEMS for participating in ancillary service markets. Ajao *et al.* [29] proposed a method of modeling a variety of household appliances and their operating constraints and formulated the design problem as a mixed-integer linear program (MILP), which minimizes its operational costs, considering V2G and V2H bidirectional flow abilities. The difference between V2G and V2H is whether it is required to consider constraints about in-home electricity or not. In [30], an optimal automated scheduling scheme was proposed, which minimizes the total operational cost satisfying various practical constraints by using forecast future market price data. In [31], a scheduling algorithm of flexible charging and discharging based on the V2H technology was proposed, which aims to use the PEV battery as energy storage in the peak power demand period. In [32], a stochastic dynamic programming framework was used for the optimal energy management of a smart home using PEV batteries and quantified the potential cost savings in various operational scenarios, including V2G, V2H, and G2V. A further design of V2H-HEMS, including a predictive model of home power demand and mobility of PEV, is described in [33]. In [34], a hybrid V2G/V2H system platform was developed for demand response in the distribution network and verified the effectiveness by showing experimental results of the implemented system. When a vehicle parked at a home contributes to the stabilization of grid power, the V2H system can be considered as a subset of H2G [35].

As far as the authors' knowledge, however, there are no works on the design of unified scheme that can provide a bidding strategy considering the consumption behavior and operating constraints of individuals and algorithm to dispatch the ancillary market signal appropriately in order to maximize users' profit. Based on this consideration, this article presents a design of new V2H-HEMS aggregator that enables each household to participate in a regulation market by adopting a multilayered control strategy that consists of MPC and real-time balancing control.

The main contribution of this article is to design an aggregator for V2H-HEMS to participate in the regulation market by considering the individual consumption behavior and various constraints. The proposed V2H-HEMS can participate in the ancillary market so that each household takes a balance of minimization of electricity charges without violating the demand on vehicle use for transportation and maximization of the profits by getting incentives for participating in the ancillary market. Comparing with the related research works introduced earlier, the merits of the proposed method are summarized as follows.

1) V2H can become a new player to participate in the ancillary service.
2) Different time-scale controls from bidding to real-time dispatching are proposed in a unified scheme.
3) Scalability is realized due to a decentralized control architecture.

The rest of this article is organized as follows. Section II describes an overview of the proposed system and the system's operation. Section III presents the formulations of the MPC models for planning the optimal power profile, aggregation, aggregator bidding, and balancing control to respond to

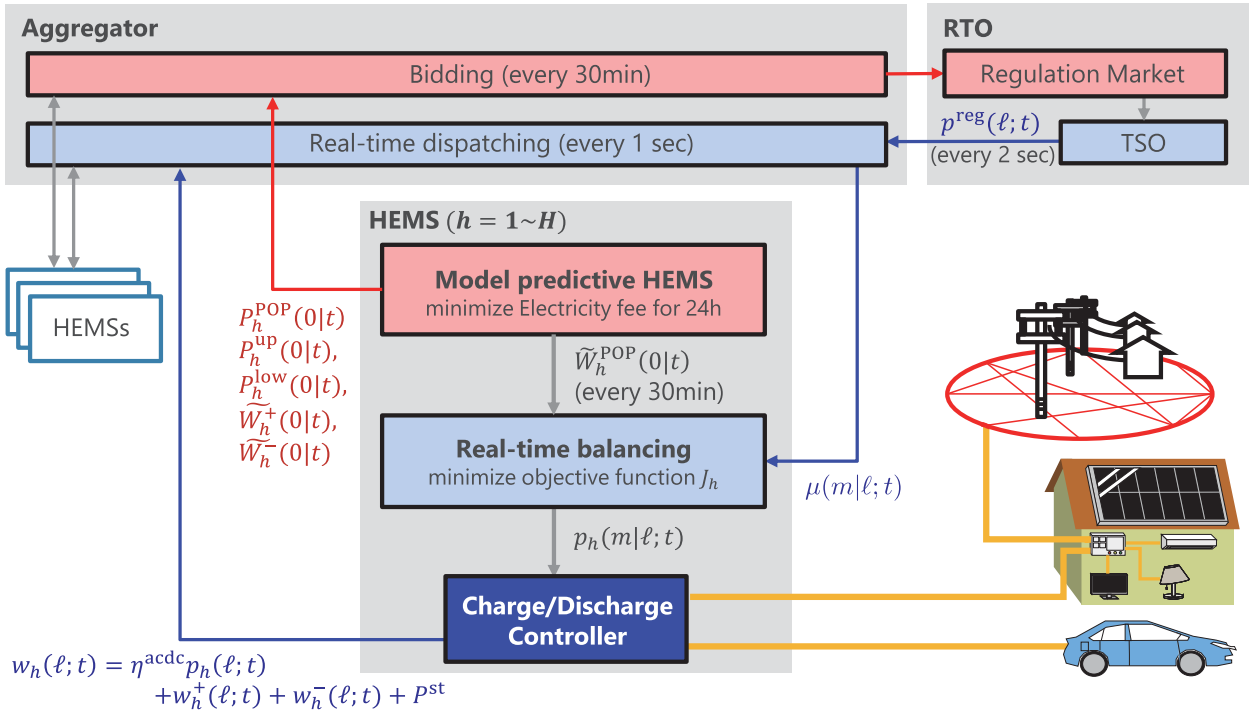

Fig. 1. System diagram of HEMS and aggregator for participation in regulation market.

regulation signals. In Section IV, evaluation of the proposed scheme based on simulation together with evaluation indices is provided. In particular, the simulation was conducted in a realistic environment by using data of power consumption and generated electric power actually measured in real households. The simulation results demonstrate the effectiveness of the proposed scheme. SectionV concludes this article.

II. Overview of the Proposed System

Fig. 1 shows a diagram of the proposed system. The system consists of multiple homes equipped with HEMSs, EVs, or PHVs, an aggregator that manages the HEMSs, and a TSO that operates a regulation market. In the system, each HEMS calculates the profiles of power capacity based on the customer's vehicle usage, household energy consumption and generation, and the customer's 24-h electric bill. The profile provides an upper and lower power bound for charging and discharging an EV or PHV. This power capacity profile is calculated every 30 [min] along with the bidding cycle. After calculation, the aggregator gathers the planned power profiles from all HEMSs and bids the total power range as a bidding capacity to the regulation market every 30 [min]. The TSO determines the regulation signals that will be used to correct small frequency deviations within the range of the bidding capacity submitted by the aggregator and sends these signals to the aggregator every 2 [s]. To follow the regulation signals, the aggregator dispatches the Lagrange multiplier to each HEMS. Each HEMS derives its target charging and discharging values based on both its internally calculated power preferred operating point (POP) and the Lagrange multiplier provided by the aggregator second by second. Finally, each HEMS charges or discharges its in-vehicle batteries using a real-time charging/discharging controller [36]. We call this system V2H rather than V2G because our algorithm never directs flows of power from the EV/PHV batteries back into the grid.

Fig. 2 shows the procedure from the scheduling to the real-time control through the first optimization of scheduling for each model predictive HEMS, the bidding capacity of HEMS aggregation, the receiving regulation signals, and the second optimization for real-time balancing with the dispatching of the request control signals to each HEMS (in the left part). The right part illustrates the different time scales corresponding to each process in the left part. Note that Problems A^{up} and A^{low} calculate the rough bidding capacity every 30 min and Problems B' and B" calculate the charging and discharging powers every 2 s to reflect the immediate change of the real power consumption in a house and the power generation by renewable energy resources. The details for these processes are described in Section III.

III. Problem Formulation

A. Derivation of Power Capacity in Model Predictive HEMS

The model predictive scheduler calculates 24-h profiles of upper and lower power bounds in 30-min intervals. The difference between the upper and lower power bounds is the power capacity, which can be submitted by the HEMS to the regulation market during the corresponding bidding time period. The profiles are based on the minimizations of cost

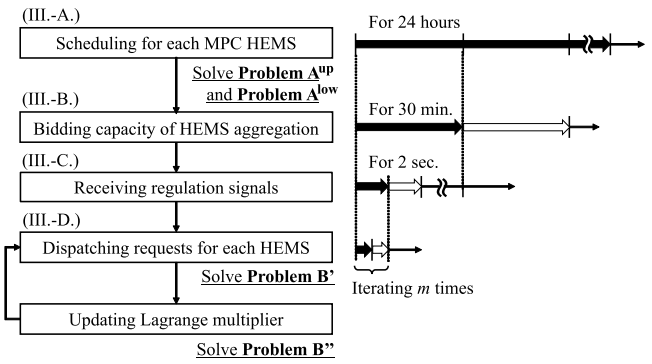

Fig. 2. Procedure of the proposed scheme from the scheduling to the control.

functions that reflect incentives and penalties for increasing each state of charge (SoC) of the in-vehicle battery. After aggregating the upper and lower power bound information from each HEMS, the aggregator bids the resulting total power range as a bidding capacity into the market.

The calculation of the profiles of upper and lower power bounds at home $h \in H$ for 24 h can be expressed in the following problems A^{up} and A^{low}, respectively:

Problem A^{up}*:*

Given $\{\tilde{W}_h^+(k|t),\ \tilde{W}_h^-(k|t),\ \tilde{\Gamma}_h(k|t),\ \tilde{P}_h^{\mathrm{cons}}(k|t),\ F^+(t+k),\ F^-(t+k)\}_{k\in[0,T-1]},\ B_h^0(t)$;

find $\left\{P_h^{\mathrm{up}}(k|t)\right\}_{k\in[0,T-1]}$;

which minimize

$$Z_h^{\mathrm{up}} = \sum_{k=0}^{T-1} F(k)\tilde{W}_h(k|t)\Delta t + \sum_{k=0}^{T-2} \alpha|P_h^{\mathrm{up}}(k|t) - P_h^{\mathrm{up}}(k+1|t)| - \sum_{k=1}^{T-1} \beta B_h(k|t),$$

$$F(k) = \begin{cases} F^+(k), & \text{if } \tilde{W}_h(k|t) \geq 0, \\ F^-(k), & \text{otherwise.} \end{cases} \tag{1}$$

subject to $\forall k \in [0, T-1]$, $s = \mathrm{up}$,

$$\tilde{W}_h(k|t) = \tilde{W}_h^+(k|t) + \tilde{W}_h^-(k|t) + P_h^s(k|t) + P^{\mathrm{st}}, \tag{2}$$

$$\tilde{W}_h(k|t) \leq W_h^{\max}, \tag{3}$$

$$\tilde{W}_h^+(k|t) + P_h^s(k|t) + P^{\mathrm{st}} \geq 0, \tag{4}$$

$$P_h^s(k|t)\tilde{\Gamma}_h(k|t) = 0, \tag{5}$$

$$P_h^{\mathrm{dis}} \leq P_h^s(k|t) \leq P_h^{\mathrm{char}}, \tag{6}$$

$$B_h^{\min} \leq B_h(k|t) \leq B_h^{\max}, \tag{7}$$

$$B_h^{\mathrm{ref}} \leq B_h(k+1|t) \quad \text{if} \quad \tilde{\Gamma}_h(k|t) = 0 \text{ and } \tilde{\Gamma}_h(k+1|t) = 1, \tag{8}$$

$$B_h(0|t) = B_h^0(t) \tag{9}$$

$$B_h(k+1|t) = B_h(k|t) - \tilde{\Gamma}_h(k|t)\tilde{P}_h^{\mathrm{cons}}(k|t)\Delta t + \left(1 - \tilde{\Gamma}_h(k|t)\right)\eta P_h^s(k|t)\Delta t, \tag{10}$$

$$\eta = \begin{cases} \eta^{\mathrm{char}}, & \text{if } P_h^s(k|t) \geq 0, \\ \eta^{\mathrm{dis}}, & \text{otherwise.} \end{cases} \tag{11}$$

Problem A^{low}*:*

Given $\{\tilde{W}_h^+(k|t),\ \tilde{W}_h^-(k|t),\ \tilde{\Gamma}_h(k|t),\ \tilde{P}_h^{\mathrm{cons}}(k|t),\ F^+(t+k),\ F^-(t+k)\}_{k\in[0,T-1]},\ B_h^0(t)$;

find $\left\{P_h^{\mathrm{low}}(k|t)\right\}_{k\in[0,T-1]}$;

which minimize

$$Z_h^{\mathrm{low}} = \sum_{k=0}^{T-1} F(k)\tilde{W}_h(k|t)\Delta t + \sum_{k=0}^{T-2} \alpha|P_h^{\mathrm{low}}(k|t) - P_h^{\mathrm{low}}(k+1|t)| + \sum_{k=1}^{T-1} \beta B_h(k|t),$$

$$F(k) = \begin{cases} F^+(k), & \text{if } \tilde{W}_h(k|t) \geq 0, \\ F^-(k), & \text{otherwise.} \end{cases} \tag{12}$$

subject to $\forall k \in [0, T-1]$, $s = \mathrm{low}$, (2)–(11).

In the cost functions (1) and (12), $\alpha|P(k|t) - P(k+1|t)|$ works to smooth the profile of charge and discharge. As a result of smoothing, frequent switching of the charging and discharging states is moderated. The terms $-\beta B_h(k|t)$ in (1) and $+\beta B_h(k|t)$ in (12) work so that the battery is charged as much or less as possible under the constraints. These terms are a new contribution comparing with our previous research [14], in which an optimal profile of charging and discharging is derived. On the contrary, to derive the profiles of upper and lower bounds of charging and discharging, these terms are added in the cost functions (1) and (12). Note that the cost functions do not include the rewards from the regulation service directory. The purpose of these cost functions is to obtain the regulation capacity as much as possible. Estimation of the rewards is possible such as in [27]. The inclusion of the rewards in the cost function is future work.

Equation (2) is the net power purchased by house h from the grid. When the net power is positive, the power purchase by h exceeds the power sold to the grid and vice versa. The constant values P^{st} indicates the standby power of the charging and discharging controllers. Equation (3) is a constraint of the upper bound, $W_h^{\max}$, of the net power for each house, which is generally specified in the contract between the house and the power supplier. Equation (4) prevents the reverse power flow from the in-vehicle battery to the grid to comply with current regulations in countries (e.g., Japan) that prohibit reverse power flow to the electric grid from batteries. By this backward flow restriction, it is possible to prevent power from flowing directly from EVs and PHVs to the grid. This is considered to lead to maintaining the quality of electricity in the grid and is a necessary constraint in some countries such as Japan. By removing this constraint, the proposed method can be applied even in countries where backward flow from a storage battery is approved. Equation (5) is a complementary condition reflecting that the in-vehicle battery can be charged or discharged only when the vehicle is parked at home. When the vehicle is at home, $\tilde{\Gamma}_h(k|t) = 0$, $P_h(k|t)$ can take arbitrary values while satisfying other constraints. When the vehicle is out of the house, $P_h(k|t)$ must be zero and $\tilde{\Gamma}_h(k|t) = 1$. Equations (6) and (7) are constraints based on the characteristics specific to the in-vehicle battery. If the SoC reaches 100% or 0%, the HEMS cannot provide a bidding capacity because the bidding capacity must have the same amounts of charging and discharging capacity from the POP value. As a result, the performance to follow the regulation signal will become worse. To avoid this situation, the upper

and lower bounds of the SoC are set as (7). Equation (8) is a constraint that indicates the user's requirements on their vehicle usage. The in-vehicle battery must be charged to at least B_h^{ref} before the user starts driving. Equations (9) and (10) correspond to the dynamics of the SoC of the in-vehicle battery. The initial value of $B_h^0(t)$ should be observed when the vehicle is parked. When the vehicle is away from the house, $B_h^0(t)$ is estimated as $B_h^0(t) = B_h(1|t-1)$ based on (10). The dynamics of the SoC described as (10) affects depending on whether or not the vehicle is parked. In addition, the coefficient η switches depending on whether charging or discharging is occurring. Although problems A^{up} and A^{low} are nonlinear optimization problems, they can be reformulated efficiently using a formulation technique for mixed logical dynamical systems in [37] (see [14] for the details).

Each HEMS calculates the POP for charging and discharging the battery as a middle value between the upper and lower power bounds as follows:

$$P_h^{\mathrm{POP}}(0|t) = \frac{P_h^{\mathrm{up}}(0|t) + P_h^{\mathrm{low}}(0|t)}{2}. \tag{13}$$

Note that this POP is not an optimal value in the meaning of minimizing the cost functions (1) or (12). This POP is employed to derive the maximum amount of bidding capacity because the bidding capacity must have equal amounts of maximum charging power and maximum discharging one.

Fig. 3 shows the capacity range of the in-vehicle battery connected to the HEMS and its POP profile limited by the upper (charging) bound $P_h^{\mathrm{up}}(0|t)$ and lower (discharging) bound $P_h^{\mathrm{low}}(0|t)$. $P_h^{\mathrm{up}}(0|t)$ and $P_h^{\mathrm{low}}(0|t)$ are obtained after solving problems A^{up} and A^{low} and twice every 30 min. The current SoC and the two bounds make a triangle, which depicts the available range for the charging/discharging of the in-vehicle battery, and the gradient of the center line from the current SoC to the scheduled POP point shows the reference power $P_h^{\mathrm{POP}}(0|t)$ in real time. The actual SoC profile is the result of the real-time balancing communicated with the HEMS and the aggregator at the phase described in Section III-D.

B. Aggregation and Bid by the Aggregator

A set of houses with a surplus capacity to submit to the regulation market at time step t can be expressed as

$$H'(t) = \left\{h \in H \,|\, P_h^{\mathrm{up}}(0|t) - P_h^{\mathrm{low}}(0|t) > 0\right\}. \tag{14}$$

Each HEMS $h \in H'(t)$ sends the following information to the aggregator: the upper and lower power bounds for 30 min from time t; $P_h^{\mathrm{up}}(0|t)$ and $P_h^{\mathrm{low}}(0|t)$; and the net electric power for 30 min to be purchased from the grid by house h if its in-vehicle battery is charged/discharged in $P_h^{\mathrm{POP}}(0|t)$:

$$\tilde{W}_h^{\mathrm{POP}}(0|t) = \tilde{W}_h^{+}(0|t) + \tilde{W}_h^{-}(0|t) + P_h^{\mathrm{POP}}(0|t) + P^{\mathrm{st}} \tag{15}$$

$\tilde{W}_h^{\mathrm{POP}}(0|t)$ is also used as the target value for balancing control.

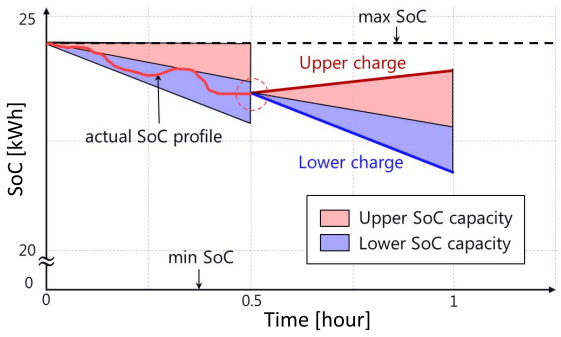

Fig. 3. POP profile of an in-vehicle battery connected to the HEMS.

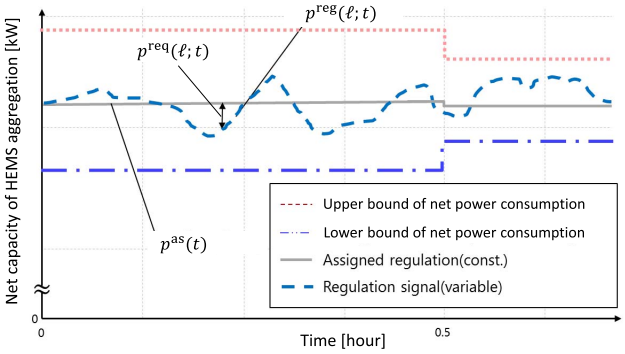

Fig. 4. Bidding capacity of charging/discharging by the HEMS aggregation.

After aggregating this information, the aggregator bids to the regulation market by sending the following information:

$$P^{\mathrm{up}}(t) = \sum_{h \in H'(t)} P_h^{\mathrm{up}}(0|t) \tag{16}$$

$$P^{\mathrm{low}}(t) = \sum_{h \in H'(t)} P_h^{\mathrm{low}}(0|t) \tag{17}$$

$$\tilde{W}^{\mathrm{POP}}(t) = \sum_{h \in H'(t)} \tilde{W}_h^{\mathrm{POP}}(0|t). \tag{18}$$

Fig. 4 shows the net charging/discharging capacity of the HEMS aggregation for all in-vehicle batteries participating in the regulation market every 30 min. The upper and lower bounds are illustrated with the red dotted line and the blue dashed–dotted line, respectively.

C. Regulation Signals From the Market to the Aggregator

The aggregator receives the regulation signals $p^{\mathrm{reg}}(\ell;t)$ from the TSO. There are two types of regulation signal: assigned regulation signals $p^{\mathrm{as}}(t)$ and regulation control signals $p^{\mathrm{req}}(\ell;t)$. The assigned regulation signal is specified as follows:

$$p^{\mathrm{as}}(t) = \tilde{W}^{\mathrm{POP}}(t). \tag{19}$$

This value is constant for 30 [min] at time step t. In practice, the regulation control signal is determined according to the condition of the market. The aggregator dispatches

$$p^{\mathrm{reg}}(\ell;t) = p^{\mathrm{as}}(t) + p^{\mathrm{req}}(\ell;t) \tag{20}$$

to each HEMS based on the balancing control, as will be described in Section III-C. Because the market is influenced by the power fluctuation on the grid due to renewable energy resources, the HEMSs can contribute to the issue of renewable energy resources if they precisely follow the regulation signal.

Please see again Fig. 4. The assigned regulation signals $p^{\mathrm{as}}(t)$ calculated by (18) are placed at the middle point in the range of the net capacity. The broken line shows an example of the regulation control signal $p^{\mathrm{req}}(\ell;t)$ sent to the HEMS aggregator from the market every 2 s.

D. Real-Time Balancing Between HEMSs and Aggregator

The primary purpose of the aggregator is to calculate the overall net power purchased from the grid by the customers following the regulation signal $p^{\mathrm{reg}}(\ell;t)$. On the other hand, from the viewpoint of each customer, the in-vehicle battery is charged/discharged according to the POP $\tilde{W}_h^{\mathrm{POP}}(0|t)$ planned by the model predictive scheduler. The balancing control accommodates the demand of each HEMS and the requirement of the aggregator.

First, the aggregator calculates the degree of contribution against the regulation for each home $h \in H'(t)$ based on [39]

$$\xi_h(t) = \frac{\sum_{h\in H'}\left(P_h^{\mathrm{up}}(0|t) - P_h^{\mathrm{low}}(0|t)\right)}{P_h^{\mathrm{up}}(0|t) - P_h^{\mathrm{low}}(0|t)}. \tag{21}$$

Then, the balancing control is formulated as the following Problem B, which is calculated by the aggregator every time instant that the regulation signal is updated.

Problem B:

Given $\{w_h^+(\ell;t),\ w_h^-(\ell;t),\ \tilde{W}_h^{\mathrm{POP}}(0|t),\ P_h^{\mathrm{up}}(0|t),\ P_h^{\mathrm{low}}(0|t)\}_{h\in H'(t)},\ p^{\mathrm{reg}}(\ell;t)$;

find $\{p_h(\ell;t)\}_{h\in H'(t)}$;

which minimize

$$J = \sum_{h\in H'(t)} \xi_h(t)\left(w_h(\ell;t) - \tilde{W}_h^{\mathrm{POP}}(0|t)\right)^2; \tag{22}$$

subject to

$$\sum_{h\in H'(t)} w_h(\ell;t) = p^{\mathrm{reg}}(\ell;t), \tag{23}$$

$$\forall h \in H'(t),$$

$$w_h(\ell;t) = w_h^+(\ell;t) + w_h^-(\ell;t) + p_h(\ell;t) + P^{\mathrm{st}}, \tag{24}$$

$$w_h(\ell;t) \le W_h^{\max}. \tag{25}$$

$$w_h^+(\ell;t) + p_h(\ell;t) + P^{\mathrm{st}} \ge 0, \tag{26}$$

$$P_h^{\mathrm{low}}(0|t) \le p_h(\ell;t) \le P_h^{\mathrm{up}}(0|t). \tag{27}$$

By minimizing the cost function (22), each model-predictive HEMS charges or discharges following the planned value while following the constraint condition (23), which is imposed to keep the overall net power purchased by the customers equal to the regulation signal. The total electric power consumed in home h at ℓ calculated using (24) is restricted by (25). The amount of charging and discharging is bounded by the upper and lower power bounds that are calculated by the model predictive scheduler in (27). Therefore, the stored energy in the battery does not exceed the lower and upper bounds of the battery capacity. The upper and lower bounds in this equation, $P_h^{\mathrm{low}}(0|t)$ and $P_h^{\mathrm{up}}(0|t)$, are derived by solving problems A^{low} and A^{up} under the constraint that the SoC does not exceed the battery capacity even if the battery is charged or discharged by the value of $P_h^{\mathrm{low}}(0|t)$ and $P_h^{\mathrm{up}}(0|t)$ for 30 [min].

Because this problem has a high computational cost when $H'(t)$ is large and is considered to take a significant amount of time to solve, it is decomposed into small problems that can be solved by each HEMS based on a dual decomposition technique [40]. In this procedure, first, Problem B is transformed into a form of dual problem with Lagrange relaxation by which the condition (23) is included in the cost function.

Problem B-dual:

Given $\{w_h^+(\ell;t),\ w_h^-(\ell;t),\ \tilde{W}_h^{\mathrm{POP}}(0|t),\ P_h^{\mathrm{up}}(0|t),\ P_h^{\mathrm{low}}(0|t)\}_{h\in H'(t)},\ p^{\mathrm{reg}}(\ell;t)$;

find $\mu(\ell;t)$;

which maximize

$$\min_{\{p_h(\ell;t)\}_{h\in H'(t)}} \left[\sum_{h\in H'(t)} \xi_h(t)\left(w_h(\ell;t) - \tilde{W}_h^{\mathrm{POP}}(0|t)\right)^2 + \mu(\ell;t)\left(\sum_{h\in H'(t)} w_h(\ell;t) - p^{\mathrm{reg}}(\ell;t)\right)\right]; \tag{28}$$

subject to

$$\forall h \in H'(t),\ (24)(26)(25)(27). \tag{29}$$

Problem B and B-dual are equivalent because of the duality theorem. By substituting (24) into (28),

$$(28) = \sum_{h\in H'(t)} \min_{p_h(\ell;t)} \left[\xi_h(t)\left(w_h(\ell;t) - \tilde{W}_h^{\mathrm{POP}}(0|t)\right)^2 + \mu(\ell;t)\,p_h(\ell;t)\right] + c\,\mu(\ell;t) \tag{30}$$

where c is a constant value, and then, this problem is decomposed to a recursive process between Problem B' for each home $h \in H'(t)$ and Problem B" for the aggregator. In the recursive procedure, the updating step is expressed by m and the charging and discharging power for each HEMS is $p_h(m|\ell;t)$, the Lagrange multiplier is $\mu(m|\ell;t)$.

Each HEMS starts to solve Problem B' with $m = 0$ with $\mu(0|\ell;t) = 0$ and sends the calculation result to the aggregator. The aggregator gathers the results of the HEMSs and updates the Lagrange multiplier $\mu(m|\ell;t)$ by Problem B", and then, it is broadcasted to each HEMS. Then, the HEMSs solve Problem B' again with incrementing m. This recursive process ends when the Lagrange multiplier converges.

Problem B':

Given $w_h^+(\ell;t),\ w_h^-(\ell;t),\ \tilde{W}_h^{\mathrm{POP}}(0|t),\ P_h^{\mathrm{up}}(0|t),\ P_h^{\mathrm{low}}(0|t),\ \mu(m|\ell;t)$;

find $p_h(m|\ell;t)$;

which minimize

$$J_h = \xi_h(t)\left(w_h(m|\ell;t) - \tilde{W}_h^{\mathrm{POP}}(0|t)\right)^2 + \mu(m|\ell;t)\,p_h(m|\ell;t); \tag{31}$$

subject to

$$\begin{aligned} &w_h(m|\ell;t) = w_h^+(\ell;t) + w_h^-(\ell;t) \\ &\qquad + p_h(m|\ell;t) + P^{\mathrm{st}}, \\ &w_h(m|\ell;t) \le W_h^{\max}, \\ &w_h^+(\ell;t) + p_h(m|\ell;t) + P^{\mathrm{st}} \ge 0, \\ &P_h^{\mathrm{low}}(0|t) \le p_h(m|\ell;t) \le P_h^{\mathrm{up}}(0|t). \end{aligned} \tag{32}$$

Problem B":
Given $\{w_h(m|\ell;t)\}_{h\in H'(t)}$, $\mu(m|\ell;t)$, $p^{\mathrm{reg}}(\ell;t)$;
find $\mu(m+1|\ell;t)$;
subject to

$$\begin{aligned} \mu(m+1|\ell;t) = \mu(m|\ell;t) \\ +\varepsilon \sum_{h\in H'(t)} \left\{ w_h(m|\ell;t) - p^{\mathrm{reg}}(\ell;t) \right\} \end{aligned} \tag{33}$$

where ε (> 0) is the parameter to adjust the speed of convergence of $\mu(m|\ell;t)$.

IV. Simulation Evaluation With Real-World Data

A. Simulation Setup

A simulation of 200 homes equipped with HEMSs as described earlier was conducted. Each household is supposed to have one EV with a 30 [kWh] capacity and a 3–5 [kW] PV cell. The simulation period was one week. In this article, the SoC is not initialized every morning. The initial value of SoC is only defined on the first day in the simulation as 50%. In order to mitigate the effect of the initial setting, the simulation was continued for one week. This setting is different from the authors' previous work [14]. The computational resources used to carry out the simulations and associated optimizations are listed in Table I.

The model predictive scheduler uses future profiles of the electric power consumed and generated in a house, represented as $\tilde{W}_h^+$ and $\tilde{W}_h^-$, respectively, $\tilde{\Gamma}_h$, a binary variable indicating whether or not the vehicle is parked, and $\tilde{P}_h^{\mathrm{cons}}$, the average electric power consumed when the vehicle is running. Such variables are usually predicted using models for, e.g., electric power consumed in a house [41], [42], electric power generated by a PV [43]–[45], and individual vehicle use [15], [16]. Note that the proposed method is applicable to a home that does not have a PV cell. In this case, we set $\tilde{W}_h^-(k|t) = 0$ and $\tilde{w}_h^-(l;t) = 0, \forall k, \forall l, \forall t$. If a stationary battery is used as an alternative for EV/PHV, we set $\tilde{\Gamma}_h(k|t) = 0, \forall k, \forall t$.

The simulations conducted in this article, however, do not use the future profiles derived from these models. Actual data obtained from real households and a statistical survey are directly used as the future profiles. This was done because the purpose of our simulation is to evaluate the possible performance of the proposed HEMS and aggregator and remove the effect of prediction error. In the authors' previous research [14], the robustness of MPC of HEMS itself is verified by using a real system and prediction error uncertainties. It is possible to discuss the robustness about MPC of Problem A in the same manner. The effect of the prediction error on the proposed system will be investigated in our future work. In the simulations conducted in this article, the aggregator bids to the regulation market by reducing the capacity by r % from the original aggregated capacity forwarded by the houses. This was done to create a more robust system for protecting the HEMS from sudden changes of available electric power in the houses. In situations of sudden change, it may not be possible to follow the regulation signal if there is a violation of the constraint conditions. The likelihood of this fault is increased if predictions of consumed and generated electric power and car use are considered. Three cases with $r = 0\%$, 10%, and 20% were examined in the simulation.

TABLE I
Computational Resources

OS	Windows 7 Professional
CPU	Intel(R) Core(TM) i7-2600S CPU@2.8GHz
Memory	8[GB]
Solver	Gurobi6.5

In this article, the regulation control signal $p^{\mathrm{req}}(\ell;t)$ is determined based on the "regulation self-test signal" [38] in the range $[P^{\mathrm{low}}(t), P^{\mathrm{up}}(t)]$ and is sent every 2 s from the aggregator. This test signal is used to check whether the client can participate in the regulation market or not. Therefore, the test signal is considered to include a certain degree of evaluation of uncertainty, though the real regulation signal will be more random.

Data on household electric power consumption and generation—respectively, $\tilde{W}_h^+(k|t)$ and $\tilde{W}_h^-(k|t)$ (sampling time 30 [min]) and $w_h^+(\ell;t)$ and $w_h^-(\ell;t)$ (sampling time 1 [sec])—was obtained from 20 real houses in Japan [46]. Using these data, 200 profiles of energy consumption and generation were constructed for various days. Profiles of car use, $\tilde{\Gamma}_h(k|t)$ (sampling time 30 [min]), were generated based on a statistical survey of car use in Japan in 2015 [47] in which users were categorized based on their primary use of their car, as shown in Tables II and III. Usage time and energy consumed by the car are listed for each category and in the category column. The average electric power consumption, $\tilde{P}_h^{\mathrm{cons}}$, was calculated by dividing the energy consumption by the car use time. The number of cars per category was derived from the population ratio obtained from the survey. Patterns of weekday and weekend use are given in Tables II and III, respectively. The electricity rates for purchasing and selling power to the grid, $F^-(t)$ and $F^+(t)$, were set to be 23.4 [JPY/kWh] and 11 [JPY/kWh] for all t [48], respectively. The purchasing electricity rate was based on a standard plan from TEPCO [49], while that for selling was based on a report on procurement price calculation produced by a committee in the Japanese Ministry of Economy, Trade and Industry. Other parameters are listed in Table IV. The parameters η^{char}, η^{dis}, and P^{st} are specified based on an experiment [14]. Generally, η^{char} is smaller than 1 because it represents the ratio of charging energy to the increment of SoC. On the other hand, η^{dis} is larger than 1 because it represents the ratio of discharging energy to the decrement of SoC. The coefficients α and β were determined empirically in this article but should be derived based on a concrete model of battery degradation. Analytical derivation of these parameters is our future work. The parameter ε was also determined empirically so that the

TABLE II
PROFILES OF CAR USE (WEEKDAY)

Category	Use time	Number of vehicles	Consumed energy by car use [kWh]	$\tilde{P}_h^{\mathrm{cons}}$ [kW]
CommutingA	8:00∼18:00	25	6	0.6
CommutingB	7:00∼17:00	20	6	0.6
CommutingC	9:00∼19:00	20	6	0.6
CommutingD	13:00∼18:00	5	3	0.6
CommutingE	14:00∼19:00	5	3	0.6
CommutingF	9:00∼12:00	5	3	1.0
CommutingG	10:00∼13:00	5	3	1.0
Leisure	-	30	0	0
ShoppingA	-	20	0	0
ShoppingB	10:00∼11:00	5	1	1.0
ShoppingC	11:00∼12:00	5	1	1.0
ShoppingD	12:00∼13:00	5	1	1.0
ShoppingE	13:00∼14:00	5	1	1.0
ShoppingF	14:00∼15:00	5	1	1.0
ShoppingG	15:00∼16:00	5	1	1.0
ShoppingH	16:00∼17:00	5	1	1.0
ShoppingI	17:00∼18:00	5	1	1.0
ShoppingJ	18:00∼19:00	5	1	1.0
ShoppingK	8:00∼9:00 18:00∼19:00	10	2	1.0
ShoppingL	7:00∼8:00 16:00∼17:00	10	2	1.0

TABLE III
PROFILES OF CAR USE (WEEKEND)

Category	Use time	Number of vehicles	Consumed energy by car use [kWh]	$\tilde{P}_h^{\mathrm{cons}}$ [kW]
CommutingA	-	25	0	0
CommutingB	-	20	0	0
CommutingC	-	20	0	0
CommutingD	-	5	0	0
CommutingE	-	5	0	0
CommutingF	-	5	0	0
CommutingG	-	5	0	0
Leisure	8:00∼20:00	30	10	0.83
ShoppingA	9:00∼15:00	20	6	1.0
ShoppingB	10:00∼11:00	5	1	1.0
ShoppingC	11:00∼12:00	5	1	1.0
ShoppingD	12:00∼13:00	5	1	1.0
ShoppingE	13:00∼14:00	5	1	1.0
ShoppingF	14:00∼15:00	5	1	1.0
ShoppingG	15:00∼16:00	5	1	1.0
ShoppingH	16:00∼17:00	5	1	1.0
ShoppingI	17:00∼18:00	5	1	1.0
ShoppingJ	18:00∼19:00	5	1	1.0
ShoppingK	8:00∼9:00 18:00∼19:00	10	2	1.0
ShoppingL	7:00∼8:00 16:00∼17:00	10	2	1.0

iteration between problems B' and B" ends in almost two rounds. Note that the large value of ε is likely to lead an undesirable oscillation in the Lagrange multiplier.

B. Evaluation Indices

The electric bill is an average fee paid by a household to the supplier of electricity that is calculated based on the electricity rates for buying and selling described in Section IV-A. Bidding capacity is calculated as $P^{\mathrm{up}}(t) - P^{\mathrm{low}}(t)$ (≥ 0). The precision rate Pr(t) [%] or ratio of the average rate for 30 [min] of actual electric power consumption over all houses, $\sum_{h\in H'(0|t)} w_h(\ell;t)$, to the regulation signal sent to the aggregator from the regulation market, $p^{\mathrm{reg}}(\ell;t) = p^{\mathrm{as}}(t) + p^{\mathrm{req}}(\ell;t)$, is calculated as follows:

$$\Pr(t) = 100\left\{1 - \frac{\frac{1}{L}\sum_{\ell=0}^{L-1} \left|\sum_{h\in H'(0|t)} w_h(\ell;t) - p^{\mathrm{reg}}(n|t)\right|}{\frac{1}{L}\sum_{\ell=0}^{L-1} |p_{\mathrm{reg}}(\ell;t)|}\right\}. \quad (34)$$

The precision rate is one of the criteria proposed by the PJM to judge the client who can participate in the regulation market [50]. The client requires scores of at least 75% in the three criteria, including the precision rate. From that viewpoint, the proposed system has enough precision rate, and however, there are penalties to a lesser or greater degree when the client cannot follow the aggregation signal. If the calculation way of the penalties is available, Problems A^{up} and A^{low} should include the penalties. This is a future work.

In the simulation, the electric bill was calculated for the three cases $r = 0\%$, 10%, and 20% and for an HEMS without an aggregator. An HEMS without an aggregator calculates the charge/discharge value $P_h^*(0|t)$ in the same manner as in Problems A^{up} and A^{low}, with the exception that $\beta = 0$ is set in (1) or (12), and calculates $p_h(\ell;t)$ as in Problem B', with the exception that $\mu(\ell;t) = 0$ is set and

$$\tilde{W}_h^{\mathrm{POP}}(0|t) = \tilde{W}_h^{+}(0|t) + \tilde{W}_h^{-}(0|t) + P_h^*(0|t) + P^{\mathrm{st}}. \quad (35)$$

TABLE IV
PARAMETERS USED IN THE SIMULATOR

Parameter	Unit	Value	Parameter	Unit	Value
$W_h^{\max}$	kW	6	η^{char}	-	0.96
P_h^{char}	kW	6	η^{dis}	-	1.04
P_h^{dis}	kW	-6	P^{st}	kW	0.155
$B_h^{\max}$	kWh	30	α	JPY/kW	0.01
$B_h^{\min}$	kWh	6	β	JPY/kWh	50
B_h^{ref}	kWh	18	ε	-	0.5

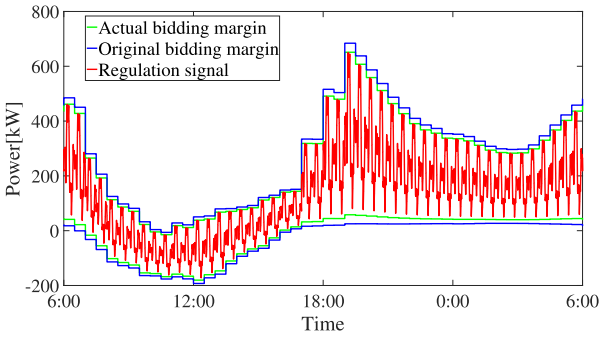

Fig. 5. Bidding capacity and regulation signal (Day 3, $r = 10\%$).

This means that an HEMS without an aggregator only attempts to determine a minimum electric bill for each house and is not rewarded for participation in the regulation market.

The reward that the aggregator received from the regulation market was estimated based on a survey of actual regulation markets [51], from which the average hourly regulation market price in the PJM in 2015 was found to be the equivalent of 3.715 [JPY/kW-h]. For example, when the aggregator submitted a capacity of 100 [kW] for 24 h, it was able to obtain $3.715 \times 100 \times 24 = 8,916$ [JPY]. The reward that the aggregator actually obtains from the regulation market depends on the precision rate, Pr(t).

C. Simulation Results

Table V shows an index of the values obtained by the simulation. As the aggregator greedily bid a larger amount of capacity when r was low, it received a higher reward from

TABLE V
EVALUATION INDICES

	HEMS with aggregator (Proposed system)			HEMS w/o aggregator
	$r = 0\%$	$r = 10\%$	$r = 20\%$	
Average bidding capacity [kW]	174	158	141	–
Electricity fee a week [JPY/house]	3,317	3,309	3,302	3,102
Estimated reward a week [JPY/house]	543	493	440	–
Total fee a week [JPY/house]	2,774	2,816	2,862	–
Average of precision rate Pr(t)[%]	94.52	95.19	95.65	–
Minimum of precision rate Pr(t)[%]	79.86	85.49	88.63	–

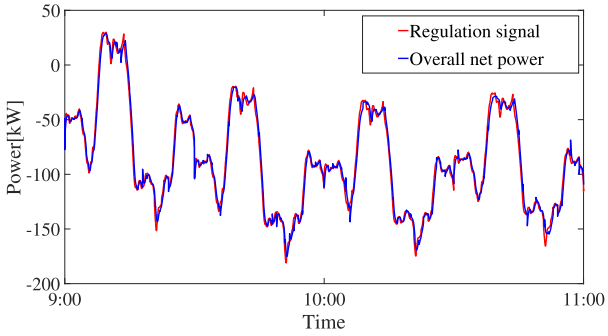

Fig. 6. Regulation signal and the overall net power of houses (9:00–11:00, Day 2, $r = 10\%$).

the regulation market. On the other hand, the electric bill increased when r was low because charging and discharging occurred at values dissimilar to $P_h^{\mathrm{POP}}(0|t)$, making the electric bill obtained by the HEMS without the aggregator lowest in this case.

The total cost is defined as the electric bill minus the estimated reward. When the reward is assumed to be evenly distributed among the HEMSs, the proposed HEMS with aggregator was more profitable than the HEMS without the aggregator. The function of an aggregator is considered to be a fund manager. Because individual HEMSs are not able to participate in the regulation market, the aggregator gathers their sources and invest them in the market. The expected reward each house receives from the aggregator is less than the estimated reward shown in Table V because the operational cost of the aggregator is not considered; estimation of the cost for operation of an aggregator is beyond the scope of this article but will be considered in future work. In addition, if the aggregator is operated by a community, the reward may be used for public services. The usage of the reward is also a key issue of the HEMS aggregator for the future.

Fig. 5 shows the regulation signals sent to the aggregator from the regulation market over the course of one day. The regulation signals change over the range of the bidding capacity with a reduction rate of $r = 10\%$. Fig. 6 shows the overall net power bought by the houses from the grid. When the net power was positive, the total power purchased from

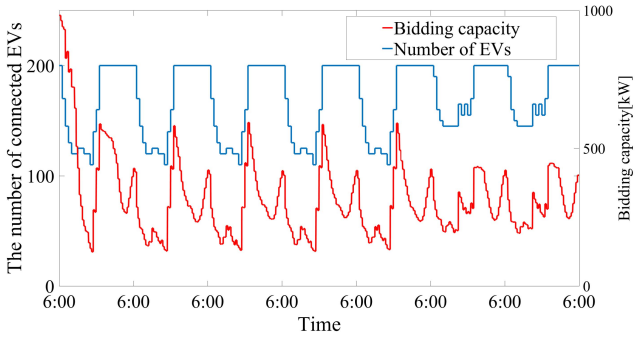

Fig. 7. Bidding capacity and number of vehicles connected to HEMS (One week, $r = 10\%$).

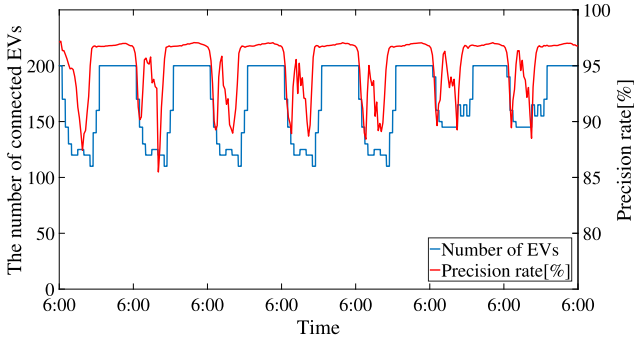

Fig. 8. Precision rate and number of vehicles connected to HEMS (One week, $r = 10\%$).

the grid exceeded the total power sold to the grid; the reverse held when the net power was negative.

As shown in Fig. 7, the amount of available capacity depended on the number of vehicles connected to the HEMSs. Fig. 8 shows that the precision rate was also affected by the total number of vehicles connected to HEMSs. This implies that the future information on the number of vehicles connected to the HEMSs is important both in calculating the capacity for bidding and for predicting the performance of the HEMSs in following the regulation signal. When the initial SoC is changed to higher or lower than 50%, the bidding capacity of the first day is only largely changed and the proposed system works successfully in the one-week simulation. The proposed system can work robustly as far as the constraints in Problems A^{up}, A^{low}, and B' are satisfied. For example, extremely low initial SoC is invalid because of the violation of constraints (6) and (7).

Figs. 9 and 10 show the SoC profiles of two of the total of 200 houses equipped with HEMS. Each house provided bidding capacity to the aggregator only when their vehicle was parked at home. In both cases, the in-vehicle batteries were correctly charged higher than $B_h^{\mathrm{ref}} = 18$ [kWh] prior to vehicle departure.

It is also seen that, over time, the electric energy of each in-vehicle battery fluctuated around the full charge state. This occurred because the lower limit value in the calculation of the minimum power capacity in Problem A^{low} cannot be reduced due to the constraint on reverse power flow (4); as a result, the POP is likely to take a value larger than zero.

Finally, the computational time of Problems B' and B" was measured. Problem B' takes average 0.44 [ms] to be solved at

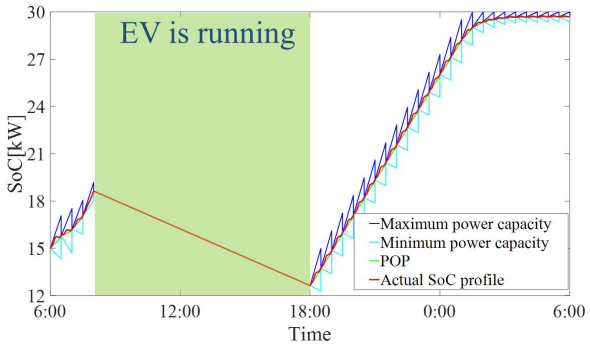

Fig. 9. SoC profile of house no. 1 (Day one, $r = 10\%$).

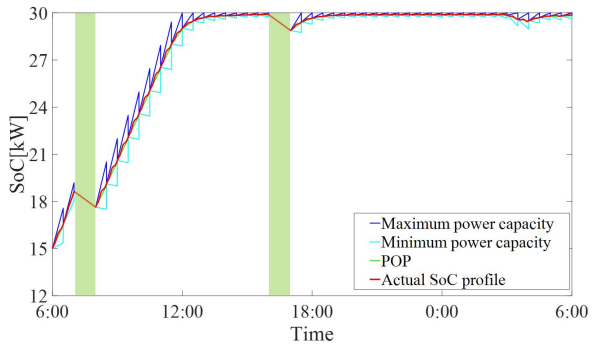

Fig. 10. SoC profile of house no. 39 (Day one, $r = 10\%$).

each household, and the calculation of Problem B" finishes in almost no time because this problem just updates the Lagrange multiplier by (33). The iteration of Problems B' and B" has converged in two or three times on average. If the round-trip communication time, delay, is assumed to be average 200 [ms] and standard deviation 20 [ms], one cycle of iteration ends in 300 [ms] at most. In this assumption, because the iteration cycle can be conducted six times in 2 s, it is enough to converge Problems B' and B". The case of Problems B' and B" not converging in six times is that there is no solution because of the constraints violation in Problem B'. Such cases are mitigated when the value of r is higher. Note that control delay in EV charging/discharging and data collection time should also be considered to implement the proposed real-time dispatch control in a real system.

V. Conclusion

In this article, an HEMS equipped with EVs and PHVs that can participate in regulation markets via an HEMS aggregator was proposed. The proposed method uses a dual composition technique to successfully reduce what would otherwise be a burdensome computational time, enabling the system to operate in conjunction with existing equipment and allowing scaling through the aggregation of large numbers of HEMSs. As TSOs require minimum capacities ranging from 100 kW to several megawatts, such aggregation of large numbers of EVs and PHVs is necessary because the individual battery capacity is limited. By including an aggregator, an average weekly saving of 491.8 JPY/house is achieved compared with the case when an aggregator is not present. In addition, the high-precision rate of 95.12% was achieved in average.

Future work will involve experimental assessment by considering the starting-up and shutting-down delays of in-vehicle batteries. Because the accuracy of response to a regulation signal is lowered by such system delays, system performance will be lowered as well, making it important to conduct assessments involving delays associated with existing equipment.

We also plan to conduct simulations using data obtained from a predictive model instead of data obtained from the field. As system effectiveness depends on the accuracy of prediction, determining the effect of such prediction on results will be important.

Acknowledgment

The authors would like to thank Dr. Stijn Vandael and Joshua Marks from the University of Delaware for providing insightful suggestions on this article in the editorial process.

References

[1] W. Kempton and J. Tomic, "Vehicle-to-grid power implementation: From stabilizing the grid to supporting large-scale renewable energy," *J. Power Source*, vol. 144, no. 1, pp. 280–294, Jun. 2005, doi: 10.1016/j.jpowsour.2004.12.022.

[2] C. Budischak, D. Sewell, H. Thomson, L. Mach, D. E. Veron, and W. Kempton, "Cost-minimized combinations of wind power, solar power and electrochemical storage, powering the grid up to 99.9% of the time," *J. Power Sources*, vol. 225, pp. 60–74, Mar. 2013, doi: 10.1016/j.jpowsour.2012.09.054.

[3] A. M. Pirbazari, "Ancillary services definitions, markets and practices in the world," in *Proc. IEEE/PES Transmiss. Distrib. Conf. Expo., Latin Amer. (T&D-LA)*, Sao Paulo, Brazil, Nov. 2010, pp. 32–36.

[4] Y. G. Rebours, D. S. Kirschen, M. Trotignon, and S. Rossignol, "A survey of frequency and voltage control ancillary services—Part I: Technical features," *IEEE Trans. Power Syst.*, vol. 22, no. 1, pp. 350–357, Feb. 2007.

[5] Y. G. Rebours, D. S. Kirschen, M. Trotignon, and S. Rossignol, "A survey of frequency and voltage control ancillary services—Part II: Economic features," *IEEE Trans. Power Syst.*, vol. 22, no. 1, pp. 358–366, Feb. 2007.

[6] J. MacDonald, P. Cappers, D. Callaway, and S. Kiliccote, "Demand response providing ancillary services a comparison of opportunities and challenges in the us wholesale markets," in *Proc. Grid-Interop*, Irving, TX, USA, Dec. 2012.

[7] Z. Zhou, T. Levin, and G. Conzelmann, "Survey of U.S. Ancillary services markets," Argonne Nat. Lab., Chicago, IL, USA, Tech. Rep. ANL/ESD-16/1, Jan. 2016.

[8] T. Bogodorova, L. Vanfretti, and K. Turitsyn, "Voltage control-based ancillary service using thermostatically controlled loads," in *Proc. IEEE Power Energy Soc. Gen. Meeting (PESGM)*, Boston, MA, USA, Jul. 2016, pp. 1–5.

[9] H. Hao, A. Kowli, Y. Lin, P. Barooah, and S. Meyn, "Ancillary service for the grid via control of commercial building HVAC systems," in *Proc. Amer. Control Conf.*, Washington, DC, USA, Jun. 2013, pp. 467–472.

[10] F. A. Qureshi, I. Lymperopoulos, A. A. Khatir, and C. N. Jones, "Economic advantages of office buildings providing ancillary services with intraday participation," *IEEE Trans. Smart Grid*, vol. 9, no. 4, pp. 3443–3452, Jul. 2018, doi: 10.1109/TSG.2016.2632239

[11] Y. Lin, P. Barooah, and J. L. Mathieu, "Ancillary services to the grid from commercial buildings through demand scheduling and control," in *Proc. Amer. Control Conf. (ACC)*, Chicago, IL, USA, Jul. 2015, pp. 3007–3012.

[12] J. Li and Z. Li, "Multi-market bidding strategy considering probabilistic real time ancillary service deployment," in *Proc. IEEE Electr. Power Energy Conf. (EPEC)*, Ottawa, ON, Canada, Oct. 2016, pp. 1–8.

[13] Agency for Natural Resources and Energy, Japan. (2018). *Power Survey Statistics, Japanese*. Accssed: Jul. 27, 2018. [Online]. Available: http://www.enecho.meti.go.jp/statistics/electric_power/ep002/pdf/2018/0-2018.pdf

[14] A. Ito, A. Kawashima, T. Suzuki, S. Inagaki, T. Yamaguchi, and Z. Zhou, "Model predictive charging control of in-vehicle batteries for home energy management based on vehicle state prediction," *IEEE Trans. Control Syst. Technol.*, vol. 26, no. 1, pp. 51–64, Jan. 2018.

[15] T. Yamaguchi, A. Kawashima, A. Ito, S. Inagaki, and T. Suzuki, "Real-time prediction for future profile of car travel based on statistical data and greedy algorithm," *SICE J. Control, Meas., Syst. Integr.*, vol. 8, no. 1, pp. 7–14, 2015.

[16] T. Yamaguchi, S. Inagaki, T. Suzuki, A. Ito, M. Fujita, and J. Kanamori, "Maximum likelihood estimation of departure and travel time of individual vehicle using statistics and dynamic programming," in *Proc. 16th Int. IEEE Conf. Intell. Transp. Syst. (ITSC)*, The Hague, The Netherlands, Oct. 2013, pp. 1674–1679.

[17] A. Kawashima, R. Sasaki, T. Yamaguchi, S. Inagaki, A. Ito, and T. Suzuki, "Energy management systems based on real data and devices for apartment buildings," in *Proc. IECON-41st Annu. Conf. IEEE Ind. Electron. Soc.*, Yokohama, Japan, Nov. 2015, pp. 3212–3217.

[18] A. Kawashima, T. Yamaguchi, R. Sasaki, S. Inagaki, T. Suzuki, and A. Ito, "Apartment building energy management system in group optimization with electricity interchange using in-vehicle batteries," *SICE J. Control, Meas., Syst. Integr.*, vol. 8, no. 1, pp. 52–60, 2015.

[19] S. Kanboj, W. Kempton, and K. Decker, "Deploying power grid-integrated electric vehicles as a multi-agent system," in *Proc. 10th Int. Conf. Auto. Agents Multiagent Syst. (AAMAS)*, Taipei, Taiwan, vol. 1, May 2011, pp. 13–20.

[20] S. Vandael, T. Holvoet, G. Deconinck, S. Kamboj, and W. Kempton, "A comparison of two GIV mechanisms for providing ancillary services at the university of delaware," in *Proc. IEEE Int. Conf. Smart Grid Commun. (SmartGridComm)*, Vancouver, BC, Canada, Oct. 2013, pp. 211–216.

[21] I. Al-Anbagi, A. Yassine, and H. T. Mouftah, "Enhancing frequency regulation coverage for electric vehicles in a smart grid environment," in *Proc. 3rd Int. Conf. Renew. Energies Developing Countries (REDEC)*, Zouk Mosbeh, Lebanon, Jul. 2016, pp. 1–5.

[22] M. Ansari, A. T. Al-Awami, E. Sortomme, and M. A. Abido, "Coordinated bidding of ancillary services for vehicle-to-grid using fuzzy optimization," *IEEE Trans. Smart Grid*, vol. 6, no. 1, pp. 261–270, Jan. 2015.

[23] F. A. S. Gil, M. Shafie-khah, A. W. Bizuayehu, and J. P. S. Catalao, "Impacts of different renewable energy resources on optimal behavior of plug-in electric vehicle parking lots in energy and ancillary services markets," in *Proc. IEEE Eindhoven PowerTech*, Eindhoven, The Netherlands, Jun. 2015, pp. 1–6.

[24] C. Peng, J. Zou, L. Lian, and L. Li, "An optimal dispatching strategy for V2G aggregator participating in supplementary frequency regulation considering EV driving demand and aggregator's benefits," *Appl. Energy*, vol. 190, pp. 591–599, Mar. 2017.

[25] H. Liu, Z. Hu, Y. Song, J. Wang, and X. Xie, "Vehicle-to-grid control for supplementary frequency regulation considering charging demands," *IEEE Trans. Power Syst.*, vol. 30, no. 6, pp. 3110–3119, Nov. 2015.

[26] S. I. Vagropoulos, D. K. Kyriazidis, and A. G. Bakirtzis, "Real-time charging management framework for electric vehicle aggregators in a market environment," *IEEE Trans. Smart Grid*, vol. 7, no. 2, pp. 948–957, Mar. 2016.

[27] R. Wang, Y. Li, P. Wang, and D. Niyato, "Design of a V2G aggregator to optimize PHEV charging and frequency regulation control," in *Proc. IEEE Int. Conf. Smart Grid Commun. (SmartGridComm)*, Vancouver, BC, Canada, Oct. 2013, pp. 127–132.

[28] R. Wang, P. Wang, and G. Xiao, "Two-stage mechanism for massive electric vehicle charging involving renewable energy," *IEEE Trans. Veh. Technol.*, vol. 65, no. 6, pp. 4159–4171, Jun. 2016.

[29] A. Ajao, H. Pourbabak, and W. Su, "Operating cost optimization of interconnected nanogrids considering bidirectional effect of V2G and V2H," in *Proc. North Amer. Power Symp. (NAPS)*, Morgantown, WV, USA, Sep. 2017, pp. 1–6.

[30] D. Guo, P. Yi, C. Zhou, and J. Wang, "Optimal electric vehicle scheduling in smart home with V2H/V2G regulation," in *Proc. IEEE Innov. Smart Grid Technol.-Asia (ISGT ASIA)*, Bangkok, Thailand, Nov. 2015, pp. 1–6.

[31] O. I. Aloqaily, I. Al-Anbagi, D. Said, and H. T. Mouftah, "Flexible charging and discharging algorithm for electric vehicles in smart grid environment," in *Proc. IEEE Wireless Commun. Netw. Conf.*, Doha, Qatar, Apr. 2016, pp. 1–6.

[32] X. Wu, X. Hu, X. Yin, and S. J. Moura, "Stochastic optimal energy management of smart home with PEV energy storage," *IEEE Trans. Smart Grid*, vol. 9, no. 3, pp. 2065–2075, May 2018.

[33] X. Wu, X. Hu, S. Moura, X. Yin, and V. Pickert, "Stochastic control of smart home energy management with plug-in electric vehicle battery energy storage and photovoltaic array," *J. Power Sources*, vol. 333, pp. 203–212, Nov. 2016.

[34] Y. Wang, O. Sheikh, B. Hu, C.-C. Chu, and R. Gadh, "Integration of V2H/V2G hybrid system for demand response in distribution network," in *Proc. IEEE Int. Conf. Smart Grid Commun. (SmartGridComm)*, Venice, Italy, Nov. 2014, pp. 812–817.

[35] C. Hertzog, *Smart Grid Dictionary Plus*. Boston, MA, USA: Cengage Learning, 2011.

[36] A. Ito and T. Shiraki, "Optimal energy storage management in DC power networks," in *Proc. IEEE Int. Conf. Smart Grid Commun. (SmartGridComm)*, Vancouver, BC, Canada, Oct. 2013, pp. 630–635.

[37] A. Bemporad and M. Morari, "Control of systems integrating logic, dynamics, and constraints," *Automatica*, vol. 35, no. 3, pp. 407–427, Mar. 1999.

[38] (2017). *Regulation Self Test Signals of Ancillary Services in PJM*. Accessed: Nov. 29, 2017. [Online]. Available: https://pjm.com/markets-and-operations/

[39] J. Kawaguchi, "Peak-cut power control via broadcast communication and parallel processing based on quadratic performance criterion," (in Japanese), in *Proc. 60th Annu. Conf. Inst. Syst., Control Inf. Eng.*, May 2016, pp. 79–83.

[40] K. Hirata, J. P. Hespanha, and K. Uchida, "Real-time pricing leading to optimal operation under distributed decision makings," in *Proc. Amer. Control Conf.*, Portland, OR, USA, Jun. 2014, pp. 1925–1932.

[41] K. Liu *et al.*, "Comparison of very short-term load forecasting techniques," *IEEE Trans. Power Syst.*, vol. 11, no. 2, pp. 877–882, May 1996.

[42] J. W. Taylor and P. E. McSharry, "Short-term load forecasting methods: An evaluation based on European data," *IEEE Trans. Power Syst.*, vol. 22, no. 4, pp. 2213–2219, Nov. 2007.

[43] R. Huang, T. Huang, R. Gadh, and N. Li, "Solar generation prediction using the ARMA model in a laboratory-level micro-grid," in *Proc. IEEE 3rd Int. Conf. Smart Grid Commun. (SmartGridComm)*, Tainan, Taiwan, Nov. 2012, pp. 528–533.

[44] C. S. Ioakimidis, S. Lopez, K. N. Genikomsakis, P. Rycerski, and D. Simic, "Solar production forecasting based on irradiance forecasting using artificial neural networks," in *Proc. IECON—39th Annu. Conf. IEEE Ind. Electron. Soc.*, Vienna, Italy, Nov. 2013, pp. 8121–8126.

[45] M. Okata, T. Nakajima, T. Inoue, T. Y. Nakajima, H. Okamoto, and K. Suzuki, "A study of the earth radiation budget in 3-D broken cloudy atmospheres by using satellite data," *J. Geophys. Res., Atmos.*, vol. 122, no. 1, pp. 443–468, 2016.

[46] Ministry of Economy, Trade and Industry, Japan. (2017). *Smart Community*. Accessed: Nov. 29, 2017. [Online]. Available: https://www.meti.go.jp/english/policy/energyenvironment/smartcommunity/

[47] Japan Automobile Manufactuers Association. (2017). *Passenger Car Market Trends in Japan: Summary of Results of JAMA's Fiscal 2015 Survey*. Accessed: Nov. 29, 2017. [Online]. Available: https://www.jama-english.jp/release/release/2016

[48] Ministry of Economy, Trade and Industry, Japanese. (2017). *Report of January, 2016, Procurement Price Calculation Committee*. Accessed: Nov. 29, 2017. [Online]. Available: https://www.meti.go.jp/committee/chotatsukakaku/pdf/0200100.pdf

[49] Tokyo Electric Power Company, Japanese. (2017). *Electricity Rate Plans, Japanese*. Accessed: Nov. 29, 2017. [Online]. Available: https://www.tepco.co.jp/jiyuuka/service/plan/kanto/standard

[50] *Energy & Ancillary Services Market Operations: PJM Manual*, document 12, 2015.

[51] (2015). *State of the Market Report for PJM, Monitoring Analytics, PJM Interconnection*. [Online]. Available: https://www.monitoringanalytics.com/reports/PJM_State_of_the_Market/2015.shtml

Hikari Nakano received the master's degree in engineering from Nagoya University, Nagoya, Japan in 2019.

She was a Research Scholar with the College of Earth, Ocean, and Environment, University of Delaware, Newark, DE, USA, from 2016 to 2018. In 2019, she joined Nuvve Corporation, San Diego, CA, USA, as an Algorithm Engineer and is currently providing professional services in vehicle-to-grid projects in Japan.

Ikumi Nawata was born in Aichi, Japan, in 1992. He received the B.S. and M.S. degrees in electronic mechanical engineering from Nagoya University, Nagoya, Japan, in 2015 and 2017, respectively.

In 2017, he joined Hitachi Ltd., Tokyo, Japan, where he is currently with the Development of Social Infrastructure Systems.

Shinkichi Inagaki (Member, IEEE) received the B.S. and M.S. degrees in electronic mechanical engineering from Nagoya University, Nagoya, Japan, in 1998 and 2000, respectively, and the Ph.D. degree in precision engineering from Tokyo University, Tokyo, Japan, in 2003.

He was an Assistant Professor from 2003 to 2008, a Lecturer from 2008 to 2015, and an Associate Professor from 2015 to 2020 with the Department of Mechanical Science and Engineering, Nagoya University. He is currently a Professor with the Department of Mechatronics, Faculty of Science and Engineering, Nanzan University, Nagoya. His current research interests are in the areas of energy management systems and decentralized control systems.

Dr. Inagaki is a member of the Society of Instrument and Control Engineers (SICE), the Robotics Society of Japan (RSJ), and the Japan Society of Mechanical Engineers (JSME).

Akihiko Kawashima (Member, IEEE) received the Ph.D. degree in engineering from Chiba University, Chiba, Japan, in 2013.

He was a Post-Doctoral Researcher from 2013 to 2015 and an Assistant Professor from 2015 to 2020 with Nagoya University, Nagoya, Japan. In 2020, he joined Yamato Holdings Company Ltd., Tokyo, Japan, where he is currently a professional worker for transportation. His research interests include combinatorial optimization, computational complexity, and its application to the design of systems for energy management and transportation.

Dr. Kawashima is a member of the Institute of Electrical Engineers of Japan (IEEJ) and the Society of Instrument and Control Engineers (SICE).

Tatsuya Suzuki (Member, IEEE) was born in Aichi, Japan, in 1964. He received the B.S., M.S., and Ph.D. degrees in electronic mechanical engineering from Nagoya University, Nagoya, Japan, in 1986, 1988, and 1991, respectively.

From 1998 to 1999, he was a Visiting Researcher with the Mechanical Engineering Department, University of California at Berkeley, Berkeley, CA, USA. He is currently a Professor with the Department of Mechanical Systems Engineering and the Executive Director of the Global Research Institute for Mobility in Society (GREMO), Nagoya University. He was a Principal Investigator with JST, CREST, Tokyo, Japan, from 2013 to 2019. His current research interests are in the areas of analysis and design of human-centric intelligent mobility systems, and integrated design of transportation and smart grid systems.

Dr. Suzuki is a member of the Society of Instrument and Control Engineers (SICE), ISCIE, IEICE, JSAE, the Robotics Society of Japan (RSJ), the Japan Society of Mechanical Engineers (JSME), and the Institute of Electrical Engineers of Japan (IEEJ). He received the Best Paper Award at the International Conference on Autonomic and Autonomous Systems in 2017, the Outstanding Paper Award at the International Conference on Control Automation and Systems in 2008, and the Journal Paper Award from IEEJ, SICE, and JSAE in 1995, 2009, and 2010, respectively.

Akira Ito (Member, IEEE) received the B.S. and M.S. degrees in electrical engineering from Osaka Prefecture University, Sakai, Japan, in 1996 and 1998, respectively, and the Ph.D. degree in mechanical science and engineering from Nagoya University, Nagoya, Japan, in 2016.

In 1998, he joined Denso Corporation, Kariya, Japan, where he is currently with the Vehicle Dynamics Engineering Division. His current research interests are in the areas of model-based systems engineering, vehicle motion control, and advanced control for autonomous vehicles.

Dr. Ito is a member of the Society of Instrument and Control Engineers (SICE) and the Japan Society of Mechanical Engineers (JSME).

Willett Kempton (Member, IEEE) is currently a Professor with the Department of Electrical and Computer Engineering and the College of Earth, Ocean, and Environment, University of Delaware, Newark, DE, USA. He directs 15 professional researchers and students in research on clean energy technologies. He invented V2G in 1997. He lectures widely and publishes scientific and technical articles on offshore wind power, electric transportation, and energy analysis.